

lncRNA-MIAT facilitates the differentiation of adipose-derived mesenchymal stem cells into lymphatic endothelial cells via the miR-495/Prox1 axis

XIAO-WEI DAI¹, WEN LUO² and CHUN-LIU LV³

¹Intensive Care Unit; ²Nuclear Medicine Department; ³Department of Breast Tumor Plastic Surgery (Third Department of Head and Neck Surgery), Hunan Cancer Hospital and The Affiliated Cancer Hospital of Xiangya School of Medicine, Central South University, Changsha, Hunan 410013, P.R. China

Received April 3, 2020; Accepted November 10, 2020

DOI: 10.3892/mmr.2021.11962

Abstract. The development of novel treatments for lymphedema is hindered by the poorly understood pathophysiology of the disease. To improve the therapeutic success of treating the disease, the present study aimed to investigate the effects and mechanism of long non-coding RNA myocardial infarction-associated transcript (MIAT) in terms of the differentiation of adipose-derived mesenchymal stem cells (ADMSCs) into lymphatic endothelial cells (LECs). The expression levels of (MIAT), microRNA (miR)-495 and Prospero-related homeobox 1 (Prox1) were measured by reverse transcription-quantitative PCR. The protein expression levels of Prox1, lymphatic vessel endothelial hyaluronan receptor 1 (LYVE-1), vascular endothelial growth factor receptor-3 (VEGFR-3) and podoplanin (PDPL) were detected by western blotting and immunofluorescence. A dual-luciferase reporter assay was also used to detect the interaction between MIAT, miR-495 and Prox1. In addition, migration and tube-formation capabilities were measured by Transwell assay and tube-formation assay, respectively. The results obtained demonstrated that VEGF-C156S (recombinant VEGF-C in which Cys156 was replaced by Ser residue) treatment could efficiently induce the differentiation of ADMSCs into LECs. MIAT expression was upregulated and miR-495 was downregulated during differentiation. Mechanistically, MIAT upregulated Prox1 expression possibly by acting as a molecular sponge for miR-495. Functional analyses indicated

that the expression levels of Prox1, LYVE-1, VEGFR-3 and PDPL, and the migration and tube-formation capabilities of ADMSCs induced by VEGF-C156S, were significantly inhibited by silencing MIAT and overexpressing miR-495. Moreover, miR-495 inhibition and Prox1 overexpression reversed the effects of MIAT downregulation and miR-495 upregulation, respectively, on the differentiation of ADMSCs into LECs. Taken together, these results suggested that MIAT may be involved in the differentiation of ADMSCs into LECs, and that the MIAT/miR-495/Prox1 axis may be a novel regulatory mechanism and therapeutic target for the treatment of lymphedema.

Introduction

Lymphedema is caused by an abnormal accumulation of fluid in interstitial tissues due to impaired fluid transport through lymphatic vasculature; it is a common form of lymphatic dysfunction and affects ~140-250 million people worldwide. Acquired lymphedema is a result of lymphatic failure caused by trauma, surgery or radiotherapy (1,2). Despite the great progress that has been made in the development of pharmacological interventions (sodium selenite, antibiotics or antifungal agents), effective therapeutic options for the treatment of lymphedema remain limited (3,4). Recent studies have suggested that promoting the regeneration of lymphatic endothelial cells (LECs) and lymphangiogenesis may effectively alleviate lymphedema (5-7). Therefore, it is essential to elucidate the physiological and molecular mechanisms of lymphangiogenesis for the development of novel and effective therapeutic targets for lymphedema.

Adipose-derived mesenchymal stem cells (ADMSCs) are mesenchymal stem cells isolated from adipose tissues that can be obtained in great quantities by minimally invasive techniques. ADMSCs have a superior multi-differentiation potential, and they have been applied in the treatment and investigation of various diseases, including lymphedema (8,9). A previous study reported that ADMSCs can be successfully induced to differentiate into LECs expressing high levels of lymphatic vessel endothelial hyaluronan receptor 1 (LYVE-1), Prospero-related homeobox 1 (Prox1) and fms-related tyrosine

Correspondence to: Dr Chun-Liu Lv, Department of Breast Tumor Plastic Surgery (Third Department of Head and Neck Surgery), Hunan Cancer Hospital and The Affiliated Cancer Hospital of Xiangya School of Medicine, Central South University, 283 Tongzipo Road, Changsha, Hunan 410013, P.R. China
E-mail: 814263506@qq.com

Key words: lymphedema, long non-coding RNA myocardial infarction associated transcript, adipose derived mesenchymal stem cells, microRNA-495, Prospero-related homeobox 1

kinase 4 (FLT-4) using a medium containing VEGF-C156S and bovine fibroblast growth factor (bFGF) (10). VEGF-C156S is a selective agonist that binds and activates VEGFR-3. However, the specific mechanism underlying how ADMSCs are differentiated into LECs has yet to be fully elucidated.

MicroRNAs (miRNAs) and long non-coding RNAs (lncRNAs) are the two main types of ncRNAs. miRNAs are small ncRNAs of ~22 nucleotides (nt) that negatively regulate gene expression by binding to the 3' untranslated regions (UTRs) of their target mRNAs, causing mRNA degradation or translational repression (11,12). lncRNAs are non-coding transcripts >200 nt in length that can act as competing endogenous RNAs (ceRNAs) to regulate the expression levels of targeted genes by sponging miRNAs, and they are involved in numerous physiological processes including cell growth, differentiation, cell proliferation and apoptosis. Previous studies have shown that lncRNA myocardial infarction-associated transcript (MIAT) has an important role in the differentiation of bone marrow mesenchymal stem cells (BM-MSCs) into endothelial cells (ECs) (13). Furthermore, Wang *et al.* (14) demonstrated that MIAT regulates VEGF by targeting miR-200a, thereby promoting the differentiation of BM-MSCs into ECs. However, little is known about the functional role and mechanism of MIAT in the differentiation of ADMSC into LECs.

In the present study, MIAT was found to be upregulated during differentiation of ADMSCs into LECs induced by VEGF-C156S, and both knockdown of MIAT and overexpression of miR-495 inhibited the differentiation of ADMSCs into LECs. Mechanistic studies revealed that MIAT could upregulate Prox1 expression by directly sponging miR-495. Therefore, the present study has newly identified an MIAT/miR-495/Prox1 axis in the differentiation of ADMSCs into LECs, thereby providing a novel avenue for lymphedema treatment.

Materials and methods

Isolation and culture of ADMSCs. All protocols were approved by the Ethics Committee of the Hunan Cancer Hospital and the Affiliated Cancer Hospital of Xiangya School of Medicine (Changsha, China). All donors gave their informed consent for harvesting of their adipose tissue; donors with malignancies, infections or systemic diseases were not included in the present study. Samples of human adipose tissue [9 females (age, 29.0±2.3 years) and 9 males (age, 31.0±1.9 years) recruited from January 2017 to December 2018] were harvested by biopsy from abdominal subcutaneous fat and washed three times with PBS. Subsequently, tissues were minced and digested with 0.75% type I collagenase (Merck KGaA) at 37°C for 1 h. After neutralization with Gibco® DMEM (Thermo Fisher Scientific, Inc.) supplemented with 10% Gibco fetal bovine serum (FBS; Thermo Fisher Scientific, Inc.), the suspension was centrifuged at 200 x g for 10 min at room temperature. The precipitate was lysed using red blood cell lysis buffer (Merck KGaA) for 10 min, followed by centrifugation at 200 x g for 10 min. The collected cells were filtered through a 150-µm nylon mesh sieve (Falcon; Corning Life Sciences) and cultured in DMEM/F12 medium (Invitrogen; Thermo Fisher Scientific, Inc.) supplemented with 10% FBS and 100 U/ml penicillin and streptomycin (Invitrogen; Thermo Fisher Scientific, Inc.)

at 37°C in an atmosphere of 5% CO₂. After 3 days, the non-adherent cells were removed, and the medium was replaced every 3 days thereafter. Cells after the third passage were used for the following experiments.

Flow cytometry analysis. ADMSC characterization was determined by flow cytometric analysis. Cultured cells were digested using 0.25% EDTA-trypsin and washed three times with PBS. After centrifugation (4°C, 300 x g for 10 min), 1x10⁴ cells/tube were incubated in the dark at room temperature for 30 min with a monoclonal APC-conjugated antibody for CD44 (1:200; clone IM7; cat. no. 560569) or with FITC-conjugated antibodies for CD105 (1:200; clone 266; cat. no. 563920), CD31 (1:100; clone WM59; cat. no. 563652) and HLA-DR (1:100; clone G46-6; cat. no. 560743); all antibodies purchased from BD Biosciences. Subsequently, the cells were washed with PBS, fixed with 4% formaldehyde and analyzed on a CytoFLEX flow cytometer and CytExpert Software 2.3 (both Beckman Coulter, Inc.).

Endothelial differentiation of ADMSCs. To induce the differentiation, ADMSCs from passage 3 were cultured in endothelial differentiation medium (EGM-2-MV; Lonza Group, Ltd.) at 37°C supplemented with 100 ng/ml VEGF-C156S (PeproTech, Inc.) for 2, 5 and 10 days, according to a previous protocol (15-17). Morphological observations were made using an inverted light microscope (TE300; Nikon).

Cell transfection. Short hairpin RNA (shRNA) against MIAT (shMIAT) and Prox1 (shProx1), an miR-495 inhibitor, miR-495 mimics and the corresponding control mimics (mimics NC; cat. no. B01001) or control inhibitor (inhibitor NC; cat. no. B03001) were designed and synthesized by Shanghai GeneChem. For Prox1 overexpression, full-length human Prox1 cDNA was cloned into the pcDNA3.1 vector (Invitrogen; Thermo Fisher Scientific, Inc.). Cells transfected with the empty pcDNA3.1 vector alone were used as a negative control. Cell transfection was performed at room temperature using Invitrogen Lipofectamine™ 3000 reagent (Thermo Fisher Scientific, Inc.), following the manufacturer's recommendations. Mimics (100 nM), inhibitors (100 nM) and shRNAs (1 µg) were added together with 1 µl Lipofectamine 3000. A second transfection was performed 6 days after the first one, following the same procedure. At day 10, cells were harvested for further experiments.

Bioinformatics analysis. The interactions between lncRNA MIAT and miR-495 were predicted by starBase v2.0 (starbase.sysu.edu.cn/index.php). The target genes of miR-495 were predicted by TargetScan Release 3.1 (targetscanmamm31/).

Luciferase reporter assay. Wild-type (WT)-MIAT, mutant type (MUT)-MIAT, WT-Prox1 and MUT-Prox1 were purchased from Hanbio Biotechnology Co., Ltd., and cloned into the luciferase reporter plasmid (psi-CHECK2; Promega Corporation). For the miR-495 and MIAT dual-luciferase reporter assay, ADMSCs were seeded into 24-well plates at a density of 1x10⁵ cells/well and cultured at 37°C for 24 h. Subsequently, ADMSCs were co-transfected with WT-MIAT or MUT-MIAT combined with miR-495 mimics,

miR-495 inhibitor or the respective negative controls using Lipofectamine® 2000 (Invitrogen; Thermo Fisher Scientific, Inc.). After 48 h, the luciferase activity was determined using a Dual Luciferase Assay System (Promega Corporation), according to the manufacturer's instructions. The interaction between miR-495 and Prox1 was verified according to the identical procedure as for miR-495 and MIAT.

Western blot analysis. Total protein was extracted from cultured cells (5×10^5 cells) using 500 μ l (1 ml/10 μ l) immunoprecipitation cell lysis buffer (cat. no. P0013; Beyotime Institute of Biotechnology) for 30 min. Afterwards, cell lysate was centrifuged at 10,000 \times g for 5 min at 4°C. Protein quantification of lysates was determined by the Bradford method (BioRad Laboratories, Inc.). Samples (30 μ g) of protein were separated by 10% SDS-PAGE and transferred onto a PVDF membrane (EMD Millipore). In order to ensure loading of the same amounts of sample, proteins of similar molecular weight to the control were not probed on the same membrane. After washing 3 times with Tris-buffered saline with 0.1% Tween-20 solution (TBST), the membranes were blocked with 5% skimmed milk for 2 h. Subsequently, membranes were incubated at 4°C overnight with primary antibodies against the following proteins: Goat polyclonal antibody against Prox1 (cat. no. AF2727; R&D Systems, Inc., 1:1,000), rabbit polyclonal antibody against LYVE-1 (cat. no. ab33682; Abcam, 1:1,000), rabbit polyclonal antibody against VEGFR3 (cat. no. ab27278; Abcam, 1:500), mouse monoclonal antibody against podoplanin (PDPL; cat. no. ab10288; Abcam, 1:1,000) and mouse monoclonal antibody against GAPDH (cat. no. ab8245; Abcam, 1:1,000). After washing with TBST, the blots were incubated with the appropriate horseradish peroxidase (HRP)-conjugated secondary antibodies (cat. nos. ab97030, ab97200 and ab97100; Abcam; 1:5,000) for 2 h at room temperature. Finally, membranes were rinsed using TBST and protein bands were subsequently visualized using chemiluminescence reagents (Immobilon; cat. no. WBKLS0500; EMD Millipore), and band densitometry were normalized to GAPDH and quantified using ImageJ software version 1.52 (National Institutes of Health).

Reverse transcription-quantitative PCR (RT-qPCR). TRIzol® reagent (Invitrogen; Thermo Fisher Scientific, Inc.) was used to isolate total RNA from cultured cells. Subsequently, cDNA was synthesized from total RNA using PrimeScript RT reagent kit (Takara Biotechnology Co., Ltd.). The expression levels of MIAT and Prox1 were detected using SYBR®-Green PCR Master mix (Thermo Fisher Scientific, Inc.), according to the manufacturer's instructions. To detect the expression of miR-495, RT was performed using TaqMan® MicroRNA Reverse Transcription kit and qPCR was performed using the TaqMan Universal Master Mix II (Applied Biosystems; Thermo Fisher Scientific, Inc.) on StepOnePlus Real-Time PCR Systems (Applied Biosystems; Thermo Fisher Scientific, Inc.). The gene expression levels were quantified using the $2^{-\Delta\Delta C_t}$ method (18). Thermocycling parameters were 94°C for 30 sec, 57°C for 30 sec and 72°C for 30 sec for 40 cycles. The primer sequences used for qPCR were as follows: GAPDH forward, 5'-GCACCGTCAAGGCTGAGAAC-3' and reverse, 5'-TGGTGAAGACGCCAGTGG-3'; U6 forward, 5'-CTC GCTTCGGCAGCACA-3' and reverse, 5'-AACGCTTCACGA

ATTTGCGT-3'; MIAT forward, 5'-ATCCTCGAGACAAAG AGCCCTCTGCACTAG-3' and reverse, 5'-ATCGGATCC GAGCAAATGGAGACAAAGGAC-3'; miR-495 forward, 5'-GCGAAACAAACATGGTGC-3' and reverse, 5'-GCA GGGTCCGAGGTATTC-3'; and Prox1 forward, 5'-CAGATG GAGAAGTACGCAC-3' and reverse, 5'-CTACTCATGAAG CAGCTCTTG-3'.

Immunofluorescence analysis. ADMSCs were grown for 72 h on glass coverslips and fixed with 4% paraformaldehyde at room temperature for 30 min. The cells were rinsed with PBS and permeabilized with 0.25% Triton X-100 in PBS for 15 min. Subsequently, the cells were incubated with a Prox1 antibody (1:500; cat. no. AF2727; R&D Systems, Inc.) resuspended in 2% BSA in PBS overnight at 4°C. After rinsing three times with PBS (10 min each wash), the cells were incubated with a secondary fluorochrome-conjugated antibody [donkey anti-goat IgG H&L (Alexa Fluor® 488); 1:1,000; cat. no. ab150132; Abcam] for 2 h in the dark. After washing with PBS, the slides were incubated with DAPI nuclear stain for 15 min. Finally, the slides were washed again and examined under an Olympus Fluoview 500 Laser Scanning Microscope (Olympus Corporation). Images were acquired from six fields of view per slide.

Transwell migration assay. Following treatment with VEGF-C156S, ADMSCs were subjected to 12 h of starvation in DMEM without serum. ADMSCs (1×10^5 cells/well) were placed into the upper chambers of Transwell inserts (8- μ m pore size; BD Biosciences). DMEM with 10% FBS was then added to the lower chambers. After 24 h of incubation at 37°C, non-migrating cells were carefully removed. The inserts were subsequently fixed with 4% paraformaldehyde and stained with 0.1% crystal violet for 30 min at room temperature. After washing with PBS, the number of migrated cells was determined using a Leica microscope, and cells were counted from five randomly selected fields using Image-Pro Plus version 6.0 software (Media Cybernetics, Inc.). Experiments were performed in triplicate.

Tube-formation assay. Twenty four-well plates were coated with ice-cold Matrigel™ solution (Phenol Red-free; BD Biosciences) and incubated at 37°C for 30 min to allow the Matrigel to solidify. Subsequently, treated ADMSCs (7×10^3 cells/well) were suspended in DMEM, seeded onto the Matrigel and incubated with normal DMEM/F12 or endothelial differentiation medium at 37°C overnight. Formation of tube-like structures was observed by phase-contrast microscopy using a Nikon Eclipse Ts2 microscope (Nikon Corporation), and the total tube length, number of tubes and area covered by tubes were quantified using ImageJ software version 1.52 (National Institutes of Health). Experiments were performed in triplicate.

Statistical analysis. All experiments were performed in triplicate and repeated three times. The results are presented as the mean \pm SD, and data were analyzed using SPSS 13.0 software (SPSS, Inc.). The normality of the data was assessed using the Shapiro-Wilk test. Considering a significance level of $P=0.05$, no significant deviations from normality were identified for

any of the data ($P > 0.05$). Statistical analyses between two groups were performed using Student's t-test, and multiple comparisons were carried out using one-way ANOVA with Tukey's post-hoc test. $P < 0.05$ was considered to indicate a statistically significant difference.

Results

Efficient differentiation of ADMSCs into LECs by VEGF-C156S treatment. Primary cultures were established from ADMSCs isolated from abdominal subcutaneous fat. Flow cytometric analysis was performed to characterize the isolated cells by examining the percentage of cells expressing four characteristic surface markers, CD44, CD105, CD31 and HLA-DR (Fig. 1A). The isolated cells were positive for CD44 and CD105 (>95% positive), which are both ADMSC markers. However, the isolated cells were negative for CD31 and HLA-DR (<2% positive), which suggested the absence of ECs and lymphocyte cells in the culture. After identification, to determine whether ADMSCs could be converted into LECs through VEGF-C156S treatment, ADMSCs were grown in EGM medium supplemented with 100 ng/ml VEGF-C156S. As early as 2 days after stimulation, the protein expression levels of multiple LEC markers, including Prox1, LYVE-1, VEGFR-3 and PDPL, were upregulated in ADMSCs, with the highest expression detected occurring at day 10 (Fig. 1B and C). These results suggested that VEGF-C156S treatment may efficiently convert the ADMSCs into LECs.

Profiling of dysregulated lncRNA-MIAT, miR-495 and Prox1 in ADMSCs during endothelial differentiation. To determine whether MIAT may be involved in the differentiation of ADMSCs into LECs, RT-qPCR was performed to evaluate the expression levels of MIAT, miR-495 and Prox1 in cells treated with VEGF-C156S for differentiation at different time points (days 0, 2, 5 and 10). The results showed that the expression levels of MIAT and Prox1 in ADMSCs were significantly increased in a time-dependent manner during VEGF-C156S treatment (Fig. 2A and C). However, the expression of miR-495 was significantly downregulated during VEGF-C156S treatment (Fig. 2B). These RT-qPCR results were further confirmed with immunofluorescence experiments, which revealed an increase in the protein expression level of Prox1 during VEGF-C156S stimulation on days 2, 5 and 10 (Fig. 2D). These results demonstrated that MIAT may have a key role in the endothelial differentiation of ADMSCs.

lncRNA-MIAT binds with miR-495 to upregulate Prox1 expression. The majority of lncRNAs function to sponge miRNAs to regulate the expression level of target genes (19); therefore, the biological associations between MIAT, miR-495 and Prox1 were further investigated. As shown in Fig. 3A, shMIAT transfection significantly decreased the expression levels of MIAT and Prox1, whereas that of miR-495 was increased compared with the shNC group. Furthermore, the expression level of miR-495 was significantly increased following transfection with miR-495 mimics and downregulated after transfection with the miR-495 inhibitor (Fig. 3B). By contrast, the expression level of Prox1 was significantly decreased after transfection with miR-495 mimics and upregulated after

transfection with the miR-495 inhibitor (Fig. 3B). Moreover, the results of a bioinformatics analysis demonstrated that there were putative binding sites there were putative binding sites for miR-495 in MIAT and miR-495 target sites in the Prox1 3'UTR (Fig. 3C and D). Furthermore, the interactions between miR-495 and MIAT, as well as between miR-495 and Prox1, were verified with dual-luciferase reporter assays. The luciferase activity in the miR-495 mimics + WT-MIAT group was significantly weaker compared with the mimics NC + WT-MIAT group; however, the luciferase activity in the miR-495 inhibitor + WT-MIAT group was significantly higher compared with that in the inhibitor NC + WT-MIAT group (Fig. 3E). However, no significant differences in the luciferase activity of MUT-MIAT were identified following treatment with the miR-495 mimics or the miR-495 inhibitor. In addition, the results of the experiment showing the interaction between miR-495 and Prox1, as confirmed by the dual-luciferase reporter assay, were consistent with the above results (Fig. 3F). Collectively, these results suggested that MIAT may enhance the expression of Prox1 by acting as a sponge for miR-495.

Knockdown of MIAT inhibits the differentiation of ADMSCs into LECs by binding miR-495. To further explore the biological function of MIAT and miR-495 in endothelial differentiation, ADMSCs exposed to VEGF-C156S were transfected with shMIAT or miR-495 mimics, or co-transfected with shMIAT and the miR-495 inhibitor, and subsequently the protein levels of Prox1, LYVE-1, VEGFR-3 and PDPL were measured by western blotting. It has previously been reported that Prox1, LYVE-1, VEGFR-3 and PDPL may be used as markers of LECs, and these are often used to assess the ability of stem cells from different sources to differentiate into LECs (20,21). Increased expression levels of Prox1, LYVE-1, VEGFR-3 and PDPL were observed in ADMSCs treated with VEGF-C156S (Fig. 4A and B). However, the expression levels of Prox1, LYVE-1, VEGFR-3 and PDPL in ADMSCs transfected with shMIAT or the miR-495 mimics were decreased compared with the control (Fig. 4A and B). Additionally, the Prox1, LYVE-1, VEGFR-3 and PDPL levels in ADMSCs inhibited by shMIAT were reversed upon co-transfection with the miR-495 inhibitor (Fig. 4A and B). To further confirm the expression of Prox1, immunofluorescence experiments were performed. Similarly, to the results from the western blotting analyses, the VEGF-C156S-induced expression of Prox1 was suppressed by MIAT silencing or miR-495 overexpression, whereas the effect of shMIAT was reversed by miR-495 knockdown (Fig. 4C). Taken together, these results indicated that MIAT silencing inhibited Prox1 expression by sponging miR-495 levels, leading to inhibited endothelial differentiation of ADMSCs.

Knockdown of MIAT inhibits migration and tube formation of ADMSCs by sponging miR-495. The migration capability of the transfected ADMSCs was measured using Transwell assays. The results indicated that knockdown of MIAT or overexpression of miR-495 inhibited the cell migration that was induced by VEGF-C156S, and co-transfection with the miR-495 inhibitor reversed the inhibition mediated by shMIAT (Fig. 5A and B). To investigate the role of MIAT and miR-495 in angiogenesis, tube-formation assays were performed. As

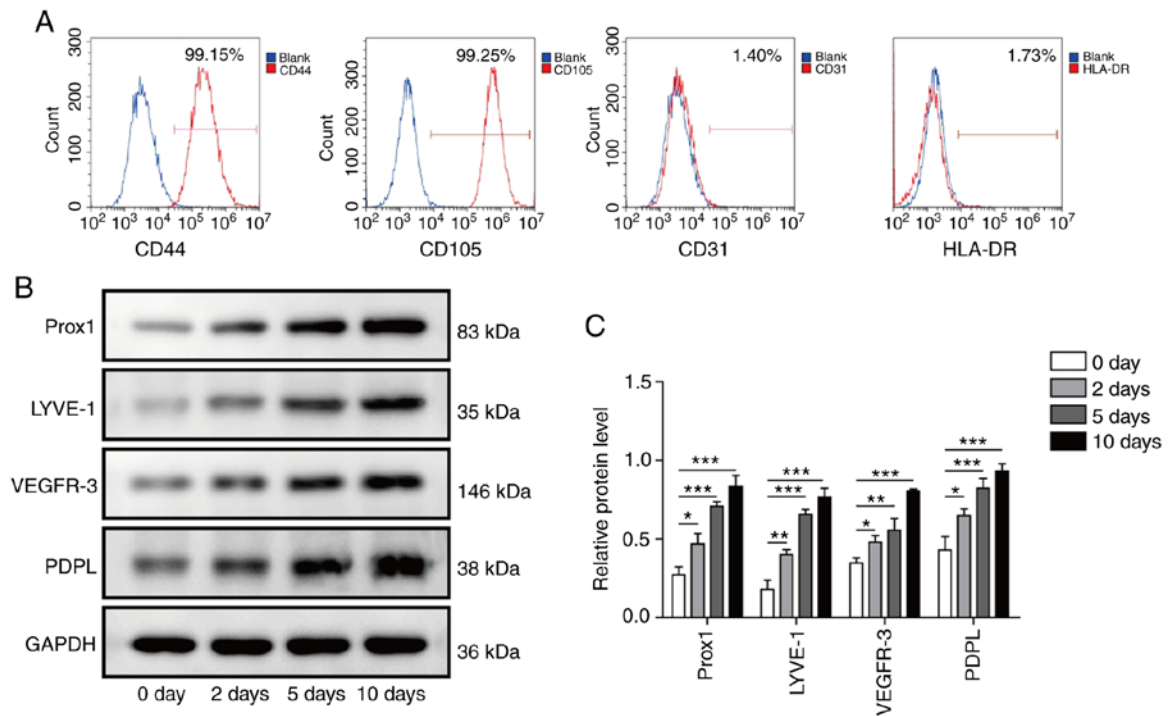


Figure 1. Characterization and endothelial differentiation of ADMSCs. (A) Flow cytometric analysis of cell surface protein expression of isolated ADMSCs. The numbers in the histograms represent the percentage of cells that were positive for the related cell surface marker. (B and C) Expression levels of Prox1, LYVE-1, VEGFR-3 and PDPL in ADMSCs treated with VEGF-C156S for 0, 2, 5 and 10 days were assessed by western blotting. All results are presented as the mean \pm SD (n=3) for three different experiments performed in triplicate. *P<0.05, **P<0.01 and ***P<0.001. ADMSC, adipose-derived mesenchymal stem cell; LYVE-1, lymphatic vessel endothelial hyaluronan receptor 1; PDPL, podoplanin; Prox1, Prospero-related homeobox 1.

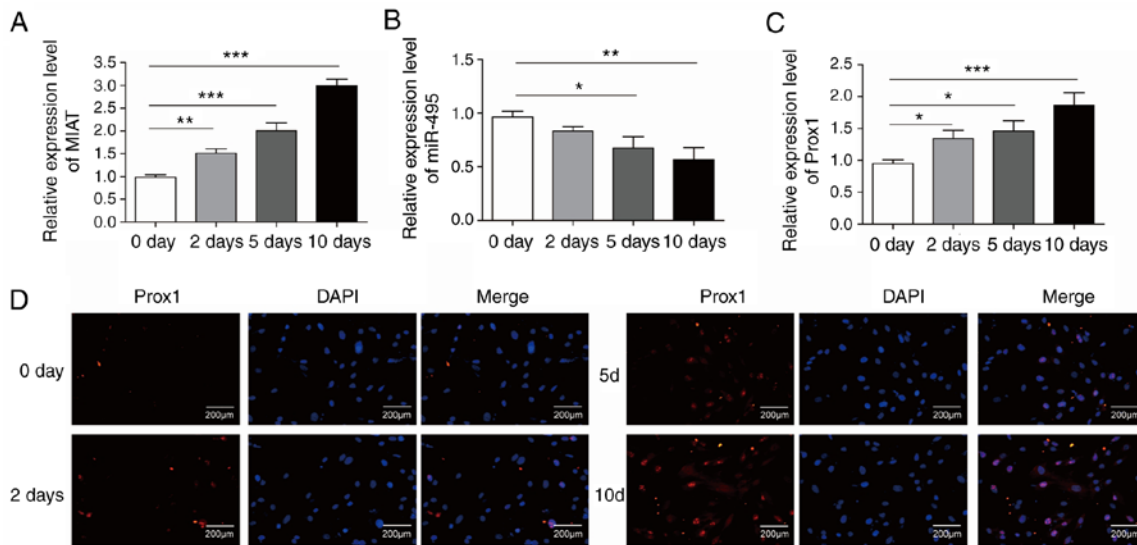


Figure 2. Expression levels of long non-coding RNA MIAT and Prox1 in ADMSCs during endothelial differentiation. The expression levels of (A) MIAT, (B) miR-495 and (C) Prox1 in ADMSCs were measured by reverse transcription-quantitative PCR at different time points during VEGF-C156S treatment (0, 2, 5 and 10 days). (D) Immunofluorescence staining of Prox1 (red) and DAPI nuclear stain (blue) in ADMSCs at different time points during VEGF-C156S treatment (0, 2, 5 and 10 days). Scale bar, 200 μ m. All results are presented as the means \pm SD (n=3) for three different experiments performed in triplicate. *P<0.05, **P<0.01 and ***P<0.001. ADMSC, adipose-derived mesenchymal stem cell; MIAT, myocardial infarction-associated transcript; miR, microRNA; Prox1, Prospero-related homeobox 1.

shown in Fig. 5C, ADMSCs treated with VEGF-C156S developed extensive capillary-like tube structures. Transfection with shMIAT or miR-495 mimics clearly inhibited the tube formation induced by VEGF-C156S treatment, whereas the inhibitory effect of shMIAT on VEGF-C156S-induced tube formation was significantly rescued by transfection of the miR-495 inhibitor

(Fig. 5C and D). Collectively, these data demonstrated that MIAT regulated migration and tube formation of ADMSCs during endothelial differentiation, likely by targeting miR-495.

miR-495 regulates VEGF-C156S-induced migration and tube formation of ADMSCs by targeting Prox1. To further delineate

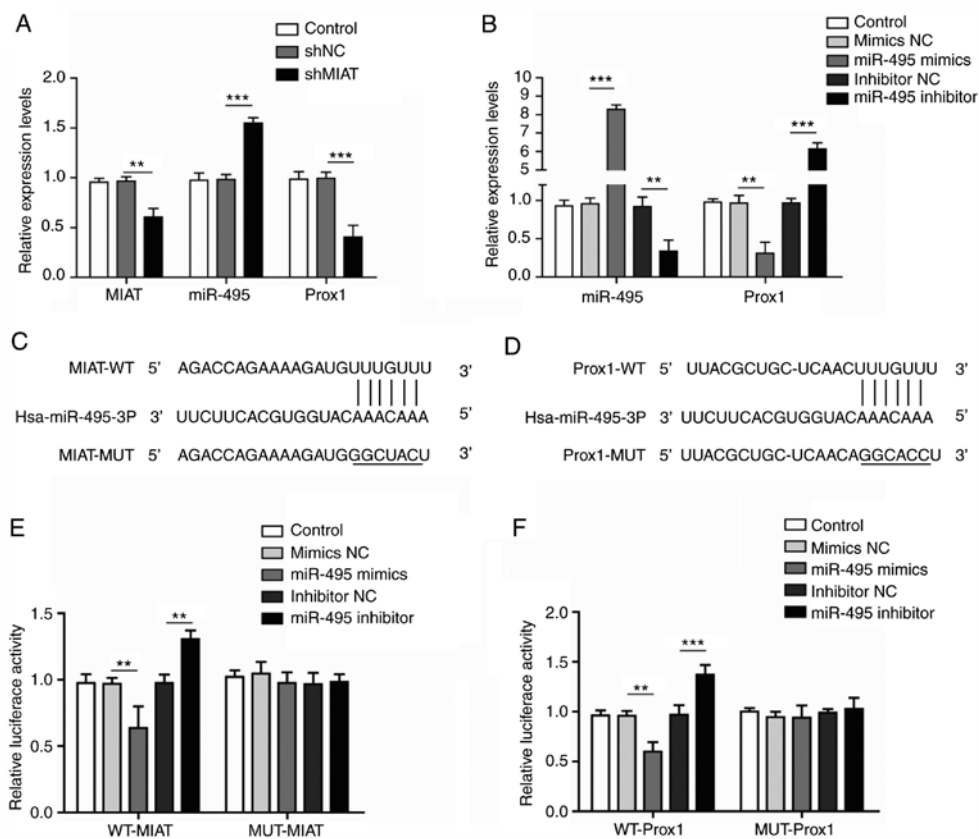


Figure 3. Long non-coding RNA MIAT negatively regulates miRNA-495 to enhance the expression of Prox1. (A) ADMSCs were transfected with shNC or shMIAT, and the expression levels of MIAT, miR-495 and Prox1 were measured by RT-qPCR. (B) ADMSCs were transfected with miR-495 mimics, miR-495 inhibitor or their respective negative controls, and the expression levels of miR-495 and Prox1 were measured by RT-qPCR. (C) StarBase analysis revealed the potential binding sites for miR-495 and MIAT. (D) StarBase analysis also revealed the potential target sites between Prox1 3'UTR and miR-495 for miR-495. (E) Luc-WT-MIAT or Luc-MUT-MIAT plasmids were co-transfected into ADMSCs with miR-495 mimics, miR-495 inhibitor or their respective negative controls, and subsequently luciferase activity was measured. (F) Luc-WT-Prox1 or Luc-MUT-Prox1 plasmids were co-transfected into ADMSCs with miR-495 mimics, the miR-495 inhibitor or their respective NCs, and luciferase activity was measured. All results are presented as the mean \pm SD (n=3) for three different experiments performed in triplicate. **P<0.01 and ***P<0.001. ADMSC, adipose-derived mesenchymal stem cell; luc, luciferase; MIAT, myocardial infarction-associated transcript; miR, microRNA; MUT, mutant type; NC, negative control; Prox1, Prospero-related homeobox 1; RT-qPCR, reverse transcription-quantitative PCR; WT, wild-type.

the effect of the miR-495/Prox1 axis on VEGF-C156S-induced migration and tube formation, a Prox1 overexpression vector and shProx1 were used. RT-qPCR analysis and western blotting revealed that the Prox1 expression levels in ADMSCs was increased following transfection with the Prox1 vector, and decreased Prox1 expression was found after transfection with shProx1 (Fig. 6A and B). Furthermore, the increases in ADMSC migration (Fig. 6C and D) and tube formation (Fig. 6E and F) induced by VEGF-C156S were inhibited by pre-transfection with shProx1. Furthermore, the inhibition of VEGF-C156S-induced migration (Fig. 6C and D) and tube formation (Fig. 6E and F) in ADMSCs induced by miR-495 mimics was also dramatically attenuated when cells were co-transfected with the Prox1 vector. Taken together, these results indicated that miR-495 may suppress the VEGF-C156S-induced migration and tube formation of ADMSCs by targeting Prox1.

Discussion

ADMSCs are accessible and abundant cells and have been used to treat lymphedema (22). It has previously been reported that VEGF-C156S-pretreated ADMSCs produced a markedly

increased lymphangiogenic response in a mouse Matrigel plug lymphangiogenesis model (15). A patient treated with ADMSCs combined with a fat-graft procedure exhibited great improvements in daily symptoms, and a reduced need for compression therapy (23). However, the underlying pathophysiological mechanisms are incompletely understood. In the present study, evidence was provided to show that MIAT exerts an important role in the process of lymphangiogenesis induced by ADMSCs. Importantly, it was shown that MIAT positively regulated the differentiation of ADMSCs into LECs by acting as a ceRNA to regulate Prox1 expression via sponging miR-495.

MSCs are multipotent cells capable of differentiating into cells of the mesodermal lineage (24). To utilize MSCs in endothelial regeneration, it is of great importance to investigate the molecular mechanisms underpinning how the differentiation of MSCs into EC-like cells is regulated. Recent studies have shown that lncRNAs may act as regulators in multiple biological processes, including MSC specification and differentiation (25,26). MIAT is considered to make important contributions to development and disease, and has been shown to facilitate the endothelial differentiation of MSCs (27,28). For example, a previous study reported

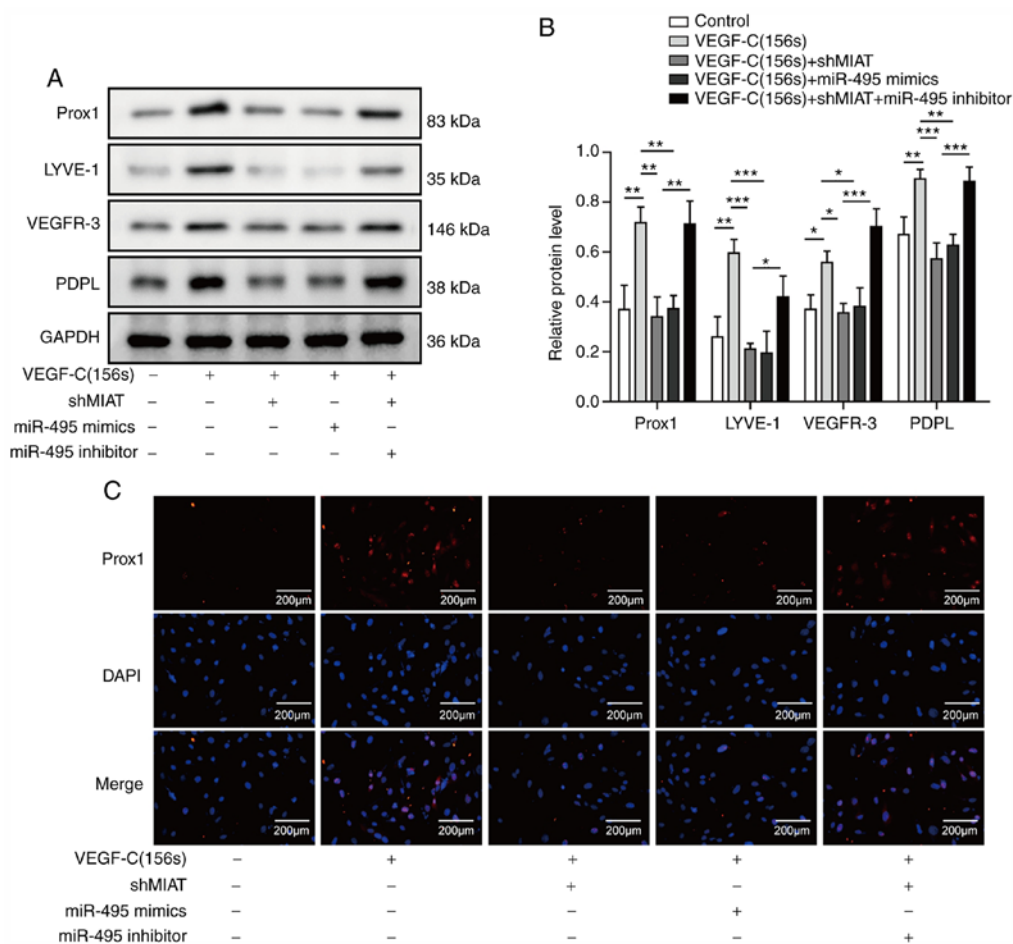


Figure 4. Long non-coding RNA MIAT knockdown inhibits LEC marker expression by sponging miR-495. ADMSCs were transfected with shMIAT or miR-495 mimics, or co-transfected with shMIAT and miR-495 inhibitor, or with shNC and control inhibitor NC or mimics NC, and the cells were incubated with VEGF-C156S for 10 days. (A and B) The protein expression levels of Prox1, LYVE-1, VEGFR-3 and PDPL were detected by western blotting. (C) Immunofluorescence staining of Prox1 (red) was measured; DAPI (blue) was used to stain the nuclei; scale bar, 200 μ m. All results are presented as the mean \pm SD (n=3) for three different experiments performed in triplicate. *P<0.05, **P<0.01 and ***P<0.001. ADMSC, adipose-derived mesenchymal stem cell; LEC, lymphatic endothelial cell; LYVE-1, lymphatic vessel endothelial hyaluronan receptor 1; MIAT, myocardial infarction-associated transcript; miR, microRNA; NC, negative control; PDPL, podoplanin; Prox1, Prospero-related homeobox 1.

that MIAT facilitated BM-MSC differentiation into ECs by regulated VEGF via targeting miR-200a (14). In addition, MIAT knockdown decreased the viability, increased the rate of apoptosis and inhibited the proliferation of ECs (29). However, the functional role of MIAT in the differentiation of ADMSCs into LECs had not been elucidated. In the present study, a marked increase in the expression of MIAT was identified in ADMSCs treated with VEGF-C156S. Furthermore, knockdown of MIAT suppressed the expression levels of Prox1 induced by VEGF-C156S and inhibited the differentiation of ADMSCs into LECs. These findings suggested that MIAT may perform crucial roles in the regulation of ADMSC differentiation into LECs.

Recently, interactions between multiple networks of lncRNA-miRNA have drawn increasing attention. Several studies have demonstrated that MIAT functions as a ceRNA to regulate cell proliferation, differentiation and angiogenesis (28,30,31). One recently published study showed that MIAT inhibited the upregulation of AKT by miR-150-5p and modulated the function and survival of human lens epithelial cells (14). It has also been reported that miR-495 can affect human umbilical vein EC proliferation and

apoptosis, promote the senescence of MSCs, and inhibit the chondrogenic differentiation of human MSCs (32-34). In the present study, markedly decreased expression levels of miR-495 were identified in ADMSCs during VEGF-C156S treatment. Furthermore, overexpression of miR-495 had an effect similar to that of MIAT silencing on the differentiation of ADMSCs into LECs. Therefore, whether MIAT could promote the endothelial differentiation of ADMSCs through miR-495 was further investigated. Bioinformatics analysis combined with a dual-luciferase reporter assay demonstrated a further sustained interaction between MIAT and miR-495. Furthermore, MIAT-inhibited ADMSCs exhibited an increase in miR-495 expression, whereas knockdown of miR-495 abolished the biological effects of shMIAT on ADMSC endothelial differentiation. These results collectively suggested that MIAT may function as a ceRNA to regulate the expression of miR-495 to promote the differentiation of ADMSCs into LECs.

Prox1 exerts a key role in the development of the mammalian lymphatic vasculature (35). In the absence of Prox1 activity, LECs were not able to be specified (36). Maintenance of the LEC phenotype requires the constant expression of

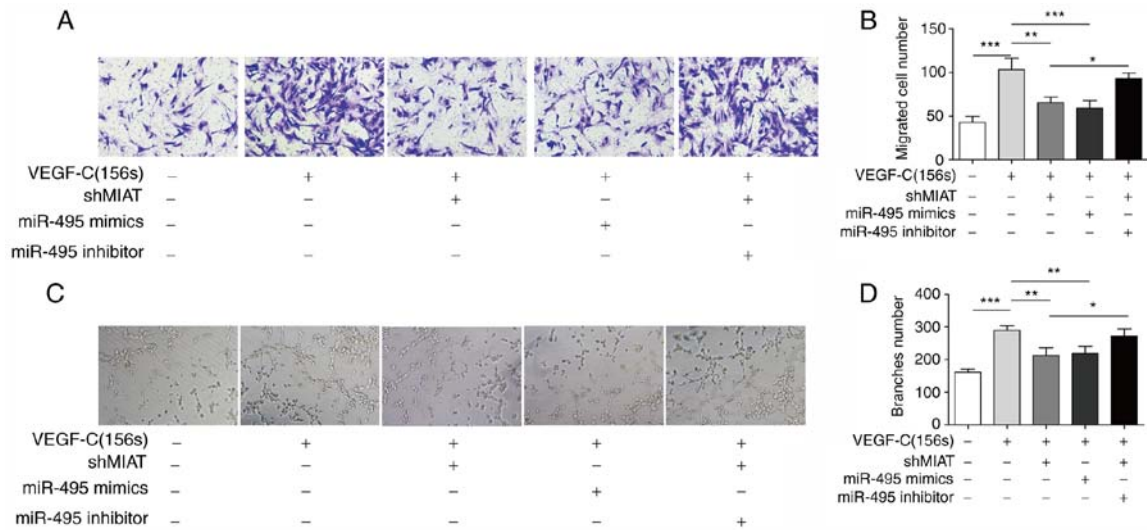


Figure 5. Long non-coding RNA MIAT knockdown inhibits migration and formation of capillary structures. ADMSCs were transfected with shMIAT, miR-495 mimics, or co-transfected with shMIAT and the miR-495 inhibitor, or with shNC and control inhibitor NC or mimics NC, and subsequently incubated with VEGF-C156S. (A and B) The migratory ability of pretreated ADMSCs was measured by Transwell assay (magnification, x100). (C and D) The capillary-like structure formation of pretreated ADMSCs was examined using tube-formation assay (magnification, x100). All results are presented as the mean \pm SD (n=3) for three different experiments performed in triplicate. *P<0.05, **P<0.01 and ***P<0.001. ADMSC, adipose-derived mesenchymal stem cell; MIAT, myocardial infarction-associated transcript; miR, microRNA; NC, negative control; sh, short hairpin RNA.

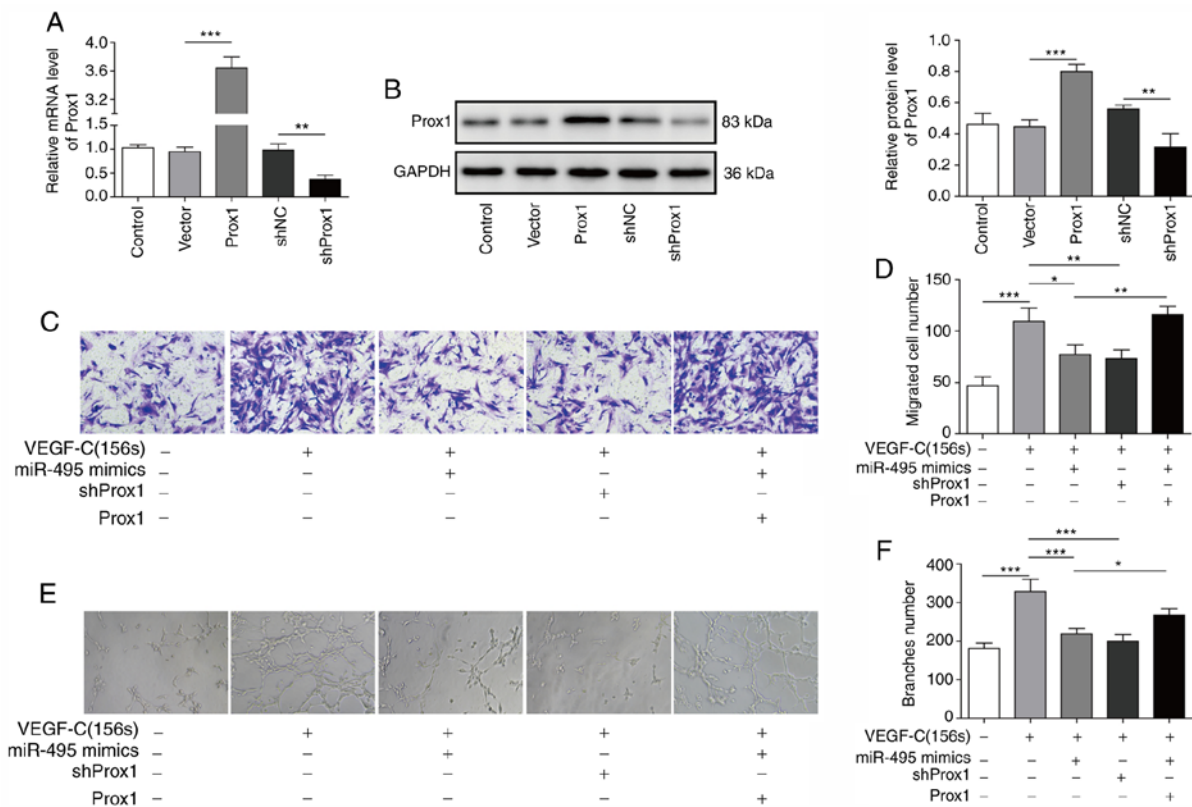


Figure 6. miR-495 regulates VEGF-C156S-induced migration and tube formation of ADMSCs by targeting Prox1. ADMSCs were transfected with the Prox1 overexpression vector, a control vector, shNC or shProx1, and subsequently the expression level of Prox1 was measured by (A) reverse transcription-quantitative PCR and (B) western blotting analysis. ADMSCs were transfected with miR-495 mimics or shProx1, or co-transfected with miR-495 mimics and the Prox1 overexpression vector, and subsequently incubated with VEGF-C156S. (C and D) The migration and (E and F) capillary-like structure formation capabilities of the cells were measured by Transwell assay and tube-formation assay, respectively. Magnification, x100. All results are presented as the mean \pm SD (n=3) for three different experiments performed in triplicate. *P<0.05, **P<0.01 and ***P<0.001. ADMSC, adipose-derived mesenchymal stem cell; miR, microRNA; Prox1, Prospero-related homeobox 1; sh, short hairpin RNA.

Prox1 (37). Moreover, several studies have confirmed that Prox1 promotes the expression of the VEGF-C receptor,

VEGFR3, and promotes lymphangiogenesis by activating VEGF-C (38,39). Consistent with these previous studies, the

present study has shown that Prox1 expression was significantly increased in ADMSCs during VEGF-C156S treatment, and knockdown of Prox1 inhibited the VEGF-C156S-induced migration and tube formation of ADMSCs. Previous studies have also suggested that lymphangiogenesis is regulated by different miRNAs through post-transcriptional regulation of Prox1 (40,41). In the present study, it was shown that miR-495 directly reduced Prox1 protein expression through binding to the 3'-untranslated region of the Prox1 mRNA. Transfection with miR-495 mimics repressed VEGF-C156S-induced tube formation and migration of ADMSCs by targeting Prox1. However, a direct interaction between VEGF-C and miR-495 was not conclusively demonstrated in the present study, and this provides a useful basis for future studies. In addition, functional experiments demonstrated that, through binding to miR-495, MIAT also indirectly regulated the expression of Prox1 in ADMSCs. Based on these results, it is possible to propose that MIAT upregulates Prox1 to promote the differentiation of ADMSCs into LECs by binding miR-495.

In conclusion, the present study has demonstrated the role of MIAT in promoting ADMSC endothelial differentiation, and has also identified a potential network by which MIAT may act as a sponge for miR-495 to regulate the expression of Prox1 in ADMSCs. Further investigation of the functional roles of MIAT may provide novel insights into developing effective treatments for lymphedema based on ADMSC transplantation.

Acknowledgements

Not applicable.

Funding

The current study was supported by Hunan Provincial Natural Science Foundation of China (grant no. 2018JJ6028).

Availability of data and materials

All data generated or analyzed during this study are included in this published article.

Authors' contributions

This study was designed by CLL. XWD collected, analyzed and ascertained the integrity and accuracy of the data. WL analyzed data and prepared the paper. All authors read approved the final manuscript.

Ethics approval and consent to participate

All protocols were approved by the Ethics Committee of the Hunan Cancer Hospital and the Affiliated Cancer Hospital of Xiangya School of Medicine (Changsha, China); and all donors gave their informed consent for the collection of their adipose tissue.

Patient consent for publication

Not applicable.

Competing interests

The authors declare that they have no competing interests.

References

- Saito Y, Nakagami H, Kaneda Y and Morishita R: Lymphedema and therapeutic lymphangiogenesis. *Biomed Res Int* 2013; 804675, 2013.
- Girgis A, Stacey F, Lee T, Black D and Kilbreath S: Priorities for women with lymphoedema after treatment for breast cancer: Population based cohort study. *BMJ* 342: d3442, 2011.
- Szuba A and Rockson SG: Lymphedema: Classification, diagnosis and therapy. *Vasc Med* 3: 145-156, 1998.
- Ko DS, Lerner R, Klose G and Cosimi AB: Effective treatment of lymphedema of the extremities. *Arch Surg* 133: 452-458, 1998.
- Karkkainen MJ, Saaristo A, Jussila L, Karila KA, Lawrence EC, Pajusola K, Bueler H, Eichmann A, Kauppinen R, Kettunen MI, *et al*: A model for gene therapy of human hereditary lymphedema. *Proc Natl Acad Sci USA* 98: 12677-12682, 2001.
- Szuba A, Skobe M, Karkkainen MJ, Shin WS, Beynet DP, Rockson NB, Dakhil N, Spilman S, Goris ML, Strauss HW, *et al*: Therapeutic lymphangiogenesis with human recombinant VEGF-C. *FASEB J* 16: 1985-1987, 2002.
- Saito Y, Nakagami H, Morishita R, Takami Y, Kikuchi Y, Hayashi H, Nishikawa T, Tamai K, Azuma N, Sasajima T and Kaneda Y: Transfection of human hepatocyte growth factor gene ameliorates secondary lymphedema via promotion of lymphangiogenesis. *Circulation* 114: 1177-1184, 2006.
- Koh KS, Oh TS, Kim H, Chung IW, Lee KW, Lee HB, Park EJ, Jung JS, Shin IS, Ra JC and Choi JW: Clinical application of human adipose tissue-derived mesenchymal stem cells in progressive hemifacial atrophy (Parry-Romberg disease) with microfat grafting techniques using 3-dimensional computed tomography and 3-dimensional camera. *Ann Plast Surg* 69: 331-337, 2012.
- Lee MJ, Kim J, Kim MY, Bae YS, Ryu SH, Lee TG and Kim JH: Proteomic analysis of tumor necrosis factor-alpha-induced secretome of human adipose tissue-derived mesenchymal stem cells. *J Proteome Res* 9: 1754-1762, 2010.
- Yang Y, Chen XH, Li FG, Chen YX, Gu LQ, Zhu JK and Li P: In vitro induction of human adipose-derived stem cells into lymphatic endothelial-like cells. *Cell Reprogram* 17: 69-76, 2015.
- He L and Hannon GJ: MicroRNAs: Small RNAs with a big role in gene regulation. *Nat Rev Genet* 5: 522-531, 2004.
- Mendell JT: MicroRNAs: Critical regulators of development, cellular physiology and malignancy. *Cell Cycle* 4: 1179-1184, 2005.
- Huang F, Fang ZF, Hu XQ, Tang L, Zhou SH and Huang JP: Overexpression of miR-126 promotes the differentiation of mesenchymal stem cells toward endothelial cells via activation of PI3K/Akt and MAPK/ERK pathways and release of paracrine factors. *Biol Chem* 394: 1223-1233, 2013.
- Wang H, Ding XG, Yang JJ, Li SW, Zheng H, Gu CH, Jia ZK and Li L: LncRNA MIAT facilitated BM-MSCs differentiation into endothelial cells and restored erectile dysfunction via targeting miR-200a in a rat model of erectile dysfunction. *Eur J Cell Biol* 97: 180-189, 2018.
- Yan A, Avraham T, Zampell JC, Haviv YS, Weitman E and Mehrara BJ: Adipose-derived stem cells promote lymphangiogenesis in response to VEGF-C stimulation or TGF- β 1 inhibition. *Future Oncol* 7: 1457-1473, 2011.
- Yan H, Zhang C, Wang Z, Tu T, Duan H, Luo Y, Feng J, Liu F and Yan X: CD146 is required for VEGF-C-induced lymphatic sprouting during lymphangiogenesis. *Sci Rep* 7: 7442, 2017.
- Yu J, Zhang X, Kuzontkoski PM, Jiang S, Zhu W, Li DY and Groopman JE: Slit2N and Robo4 regulate lymphangiogenesis through the VEGF-C/VEGFR-3 pathway. *Cell Commun Signal* 12: 25, 2014.
- Livak KJ and Schmittgen TD: Analysis of relative gene expression data using real-time quantitative PCR and the 2(-Delta Delta C(T)) method. *Methods* 25: 402-408, 2001.
- Sun X, Huang T, Zhang C, Zhang S, Wang Y, Zhang Q and Liu Z: Long non-coding RNA LINC00968 reduces cell proliferation and migration and angiogenesis in breast cancer through up-regulation of PROX1 by reducing hsa-miR-423-5p. *Cell Cycle* 18: 1908-1924, 2019.

20. Wu JK, Kitajewski C, Reiley M, Keung CH, Monteagudo J, Andrews JP, Liou P, Thirumoorthi A, Wong A, Kandel JJ and Shawber CJ: Aberrant lymphatic endothelial progenitors in lymphatic malformation development. *PLoS One* 10: e0117352, 2015.
21. Deng J, Dai T, Sun Y, Zhang Q, Jiang Z, Li S and Cao W: Overexpression of Prox1 induces the differentiation of human adipose-derived stem cells into lymphatic endothelial-like cells in vitro. *Cell Reprogram* 19: 54-63, 2017.
22. Hwang JH, Kim IG, Lee JY, Piao S, Lee DS, Lee TS, Ra JC and Lee JY: Therapeutic lymphangiogenesis using stem cell and VEGF-C hydrogel. *Biomaterials* 32: 4415-4423, 2011.
23. Toyserkani NM, Jensen CH, Sheikh SP and Sørensen JA: Cell-assisted lipotransfer using autologous adipose-derived stromal cells for alleviation of breast cancer-related lymphedema. *Stem Cells Transl Med* 5: 857-859, 2016.
24. Uccelli A, Moretta L and Pistoia V: Mesenchymal stem cells in health and disease. *Nat Rev Immunol* 8: 726-736, 2008.
25. Sun X, Luo LH, Feng L and Li DS: Down-regulation of lncRNA MEG3 promotes endothelial differentiation of bone marrow derived mesenchymal stem cells in repairing erectile dysfunction. *Life Sci* 208: 246-252, 2018.
26. Hou J, Wang L, Wu Q, Zheng G, Long H, Wu H, Zhou C, Guo T, Zhong T, Wang L, *et al*: Long noncoding RNA H19 upregulates vascular endothelial growth factor A to enhance mesenchymal stem cells survival and angiogenic capacity by inhibiting miR-199a-5p. *Stem Cell Res Ther* 9: 109, 2018.
27. Ishii N, Ozaki K, Sato H, Mizuno H, Saito S, Takahashi A, Miyamoto Y, Ikegawa S, Kamatani N, Hori M, *et al*: Identification of a novel non-coding RNA, MIAT, that confers risk of myocardial infarction. *J Hum Genet* 51: 1087-1099, 2006.
28. Sun C, Huang L, Li Z, Leng K, Xu Y, Jiang X and Cui Y: Long non-coding RNA MIAT in development and disease: A new player in an old game. *J Biomed Sci* 25: 23, 2018.
29. Yan B, Yao J, Liu JY, Li XM, Wang XQ, Li YJ, Tao ZF, Song YC, Chen Q and Jiang Q: lncRNA-MIAT regulates microvascular dysfunction by functioning as a competing endogenous RNA. *Circ Res* 116: 1143-1156, 2015.
30. Huang X, Gao Y, Qin J and Lu S: lncRNA MIAT promotes proliferation and invasion of HCC cells via sponging miR-214. *Am J Physiol Gastrointest Liver Physiol* 314: G559-G565, 2018.
31. Zhou X, Zhang W, Jin M, Chen J, Xu W and Kong X: lncRNA MIAT functions as a competing endogenous RNA to upregulate DAPK2 by sponging miR-22-3p in diabetic cardiomyopathy. *Cell Death Dis* 8: e2929, 2017.
32. Liu D, Zhang XL, Yan CH, Li Y, Tian XX, Zhu N, Rong JJ, Peng CF and Han YL: MicroRNA-495 regulates the proliferation and apoptosis of human umbilical vein endothelial cells by targeting chemokine CCL2. *Thromb Res* 135: 146-154, 2015.
33. Li X, Song Y, Liu D, Zhao J, Xu J, Ren J, Hu Y, Wang Z, Hou Y and Zhao G: MiR-495 promotes senescence of mesenchymal stem cells by targeting Bmi-1. *Cell Physiol Biochem* 42: 780-796, 2017.
34. Lee S, Yoon DS, Paik S, Lee KM, Jang Y and Lee JW: microRNA-495 inhibits chondrogenic differentiation in human mesenchymal stem cells by targeting Sox9. *Stem Cells Dev* 23: 1798-1808, 2014.
35. Choi I, Lee S and Hong YK: The new era of the lymphatic system: No longer secondary to the blood vascular system. *Cold Spring Harb Perspect Med* 2: a006445, 2012.
36. Hong YK, Foreman K, Shin JW, Hirakawa S, Curry CL, Sage DR, Libermann T, Dezube BJ, Fingerroth JD and Detmar M: Lymphatic reprogramming of blood vascular endothelium by Kaposi sarcoma-associated herpesvirus. *Nat Genet* 36: 683-685, 2004.
37. Johnson NC, Dillard ME, Baluk P, McDonald DM, Harvey NL, Frase SL and Oliver G: Lymphatic endothelial cell identity is reversible and its maintenance requires Prox1 activity. *Genes Dev* 22: 3282-3291, 2008.
38. Park YL, Myung E, Park SY, Kim N, Oak CY, Myung DS, Cho SB, Lee WS, Kweon SS, Kim HS and Joo YE: Impact of prospero homeobox-1 on tumor cell behavior and prognosis in colorectal cancer. *Am J Cancer Res* 5: 3286-3300, 2015.
39. Sasahira T, Ueda N, Yamamoto K, Kurihara M, Matsushima S, Bhawal UK, Kirita T and Kuniyasu H: Prox1 and FOXC2 act as regulators of lymphangiogenesis and angiogenesis in oral squamous cell carcinoma. *PLoS One* 9: e92534, 2014.
40. Xu C, Zhang Y, Wang Q, Jiang J, Gao Y, Gao M, Kang J, Wu M, Xiong J, Ji K, *et al*: Long non-coding RNA GAS5 controls human embryonic stem cell self-renewal by maintaining NODAL signalling. *Nat Commun* 7: 13287, 2016.
41. Ramos AD, Andersen RE, Liu SJ, Nowakowski TJ, Hong SJ, Gertz C, Salinas RD, Zarabi H, Kriegstein AR and Lim DA: The long noncoding RNA Pnky regulates neuronal differentiation of embryonic and postnatal neural stem cells. *Cell Stem Cell* 16: 439-447, 2015.